

N1-methylnicotinamide ameliorates insulin resistance in skeletal muscle of type 2 diabetic mice by activating the SIRT1/PGC-1 α signaling pathway

YU CHEN, JINGFAN ZHANG, PING LI, CONG LIU and LING LI

Department of Endocrinology, Shengjing Hospital of China Medical University, Shenyang, Liaoning 110004, P.R. China

Received June 11, 2020; Accepted October 29, 2020

DOI: 10.3892/mmr.2021.11909

Abstract. Insulin resistance is one of important factors causing type 2 diabetes; therefore, regulating insulin sensitivity is considered a beneficial therapeutic approach against type 2 diabetes. The present study aimed to determine the effects of N1-methylnicotinamide (MNAM) on insulin resistance (IR) in skeletal muscle from a mouse model of type 2 diabetes mellitus (T2DM), and to investigate the regulatory mechanisms of the sirtuin 1 (SIRT1)/peroxisome proliferator-activated receptor γ coactivator-1 α (PGC-1 α) signaling pathway. C57BL/6 mice were fed a normal diet with or without 1% MNAM and ob/ob mice were also fed a normal diet with or without 0.3 or 1% MNAM. Blood glucose, insulin levels, insulin resistance (IR), sensitivity indices and triglyceride (TG) content were detected using ELISAs. The expression of gluconeogenesis-related, insulin signaling-related and SIRT1/PGC-1 α pathway-related proteins was analyzed using reverse transcription-quantitative PCR (RT-qPCR) and western blotting. *In vitro*, C2C12 cells were used to establish an IR muscle cell model by 0.75 mM palmitic acid (PA) treatment (PA group). The IR cell model was subsequently supplemented with 1 mM MNAM (PM group) or 1 mM MNAM + 30 μ M SIRT1 inhibitor, EX527 (PME group). After treatment the glucose levels and insulin signaling-related proteins were detected by ELISAs and western blotting, respectively. Furthermore, the expression levels of SIRT1/PGC-1 α signaling pathway-related mRNA and proteins under MNAM treatment were detected by RT-qPCR and western blotting. MNAM reduced body weight gain in T2DM mice, decreased fasting blood glucose and fasting insulin levels, and inhibited IR. MNAM also regulated insulin signal transduction and promoted glucose utilization in skeletal muscle, and reduced lipid deposition. Thus, MNAM

improved IR in the skeletal muscle of T2DM mice. Following application of a SIRT1 inhibitor, the effects of MNAM on the increased glucose utilization in insulin-resistant myocytes and the insulin signaling pathway were suppressed. The mechanism of action was associated with activation of the SIRT1/PGC-1 α signaling pathway, which promoted the activation of the insulin receptor substrate IRS1/PI3K/AKT pathway.

Introduction

Diabetes is a chronic disease with worldwide distribution that occurs when insufficient insulin is produced by the pancreas, or insulin utilization in the body is defective (1). At present, there are ~463 million (9.3%) adults ranging from 20-79 years old who have been diagnosed with diabetes, of which 90% have type 2 diabetes mellitus (T2DM) (2). The two main mechanisms that result in T2DM are insulin resistance (IR) and insulin secretory dysfunction (3). Skeletal muscle is the most essential tissue that maintains glucose homeostasis in the body (4). Under normal conditions, skeletal muscle is responsible for 80% of the insulin-induced glucose uptake and utilization of the whole body (5). During IR, the expression of proteins involved in GLUT4 translocation machinery in the muscle was reported to impact glucose uptake (6). Insulin in the muscle closely coordinates GLUT4 with insulin receptor substrate 1 (IRS1), PI3K and AKT (7).

Nicotinamide (NAM) is the precursor of nicotinamide adenine dinucleotide (NAD⁺), which is widely involved in the regulation of energy metabolism, physiological rhythms and the cellular redox state (8). NAM has been reported to induce adverse effects; its 50% lethal dose (LD50) was reported to be 2.5 g/kg via oral administration and 2.05 g/kg via intraperitoneal administration in mice, with slightly higher LD50s in rats (9). NAM can be transformed into N1-methylnicotinamide (MNAM) after being methylated by nicotinamide N-methyltransferase (10). MNAM is the urinary excretory form of NAM and one of the catabolic metabolites of NAM, suggesting that MNAM is soluble in water and easy to be excluded with urine (9). MNAM possesses several protective physiological properties, including antithrombotic and anti-inflammatory effects, as well as providing protection in the vascular system (10). Previous studies have reported that MNAM can reduce fasting blood glucose (FBG) and fasting insulin (FINS) levels in mice fed with a saturated-fat diet (11).

Correspondence to: Dr Ling Li, Department of Endocrinology, Shengjing Hospital of China Medical University, 36 Sanhao Street, Heping, Shenyang, Liaoning 110004, P.R. China
E-mail: liling@sj-hospital.org

Key words: type 2 diabetes mellitus, skeletal muscle, insulin resistance, N1-methylnicotinamide, sirtuin 1/peroxisome proliferator-activated receptor γ coactivator-1 α signaling pathway

MNAM can also improve IR, which has the potential to be useful in the prevention or treatment of T2DM (12). However, the mechanisms via which MNAM affects IR are not fully understood.

Sirtuin 1 (SIRT1) is an NAD⁺-dependent deacetylase that is involved in insulin signal transduction in the regulation of glycolipid metabolism (13). MNAM was reported to regulate nutritional metabolism in liver via SIRT1 (11). One of the downstream regulators of SIRT1 is peroxisome proliferator-activated receptor γ coactivator-1 α (PGC-1 α) (14). PGC-1 α is a transcriptional coactivator that regulates mitochondrial biosynthesis and respiration, and is reported to be involved in a wide range of metabolic pathways (15). A saturated-fat diet has been reported to induce IR and decrease PGC-1 α expression in muscle tissue (16). It has been hypothesized that enhanced PGC-1 α activity may protect the body from lipid-induced IR (17). The aim of the present study was to establish a mouse model of T2DM to observe the effects of MNAM on IR and glucose metabolism. Additionally, an *in vitro* IR model was established in muscle cells to further explore the effects of MNAM on IR in skeletal muscle and the regulatory mechanism of the SIRT1/PGC-1 α signaling pathway.

Materials and methods

Establishment of T2DM mouse model. A total of 20 specific pathogen-free-grade C57BL/6 mice and 30 ob/ob mice (males; weight, 20 \pm 5 g; age, 6-8 weeks) were purchased from Beijing HFK Bio-Technology Co., Ltd. The animal experiments were conducted in the Shengjing Hospital of China Medical University. All mice were fed the standard laboratory diet for four weeks. Body weights and FBG were measured weekly. When the FBG of the ob/ob mice was >13.8 mmol/l, and the FBG and body weights were higher than those of C57BL/6 mice, the T2DM model was considered to be established successfully (18). The experimental protocols were approved by the Animal Ethics Committee of Shengjing Hospital of China Medical University (approval no. 2016PS340K).

Experimental animal grouping and treatment. Mice were randomly divided into the following groups (10 mice/group): C57BL/6 mice fed normal diet (control group); C57BL/6 mice fed MNAM (Sigma-Aldrich; Merck KGaA) at a high dose (1%; CMNAMH group); ob/ob T2DM model mice fed normal diet (DM group); T2DM mice fed with MNAM at a low dose (0.3%; DMNAML group); and T2DM mice fed with MNAM at a high dose (1%; DMNAMH group). Mice in each group were fed with their respective diets continuously for 8 weeks. The body weights and FBG were measured every 2 weeks after fasting for 12 h. Blood was collected from the tip of the tail, and FBG was measured using a CONTOUR[®]PLUS Blood Glucose Monitoring System 7600P (Bayer AG). Finally, mice were anesthetized with 1% pentobarbital sodium (45 mg/kg) and sacrificed via exsanguination, with blood collected from the abdominal aorta.

Determination of IR and sensitivity indices. An insulin ELISA kit (cat. no. CEA448Mu; Wuhan USCN Business Co., Ltd.) was used to detect the FINS level in the serum from each group according to the manufacturer's instructions. The

serum was isolated from the blood through centrifugation at 200 x g for 10 min at 4°C. The IR indices were calculated according to the results and the equations of FBG and FINS as follows: Homeostatic model assessment for insulin resistance (HOMA-IR): HOMA-IR = [FBG (mmol/l) x FINS (mIU/l)]/2.5 (19); Quantitative insulin resistance check index (QUICKI): QUICKI = 1/[log FBG (mg/dl) + log FINS (mIU/l)] (20).

Determination of triglyceride (TG) content. A TG ELISA kit (cat. no. CEB687Ge; Wuhan USCN Business Co., Ltd.) was used to determine the TG content in gastrocnemius muscle according to the manufacturer's protocols. Samples were assayed using a model 680 microplate reader (Bio-Rad Laboratories, Inc.); the TG content was calculated according to a standard curve.

In vitro experiments. C2C12 cells, an immortalized mouse myoblast cell line originally obtained by Yaffe and Saxel (21), were used for the *in vitro* experiments. C2C12 cells were purchased from the American Type Culture Collection and cultured in high-glucose DMEM (HyClone; Cytiva) supplemented with 10% FBS (HyClone; Cytiva). When the cells reached a logarithmic growth stage, the DMEM was supplemented with 2% horse serum (Sigma-Aldrich; Merck KGaA) to induce differentiation. Cells were collected when 90% cells were differentiated into myotubes. The experimental groups included a blank control group (control group), cells supplemented with 0.75 mM palmitic acid (PA) to establish an IR muscle cell model (PA group), cells supplemented with 0.75 mM PA + 1 mM MNAM (PM group), and cells supplemented with 0.75 mM PA + 1 mM MNAM + 30 μ M SIRT1 inhibitor, EX527 (Sigma-Aldrich; Merck KGaA) (PME group). Cells were incubated at 37°C in 5% CO₂ for 16 h, and then 100 nmol/l insulin was added 10 min before the cells were harvested.

Detection of residual glucose content. Following treatment of cells under each of the aforementioned conditions, 2 μ l supernatant was taken and added to 98 μ l deionized water. According to the manufacturer's instructions (cat. no. BC2500; Beijing Solarbio Science & Technology Co., Ltd.), the glucose content was calculated by detecting the absorbance at 505 nm using a microplate reader.

Reverse transcription-quantitative (RT-q)PCR. The relative mRNA levels of SIRT1 and PGC-1 α in skeletal muscle and C2C12 cells were determined using RT-qPCR. Primers were designed using DNASTAR v8.1 (www.dnastar.com) according to the sequence information published in GenBank (Table I). Total RNAs from tissues or cells were extracted using TRIzol[®] (Invitrogen; Thermo Fisher Scientific, Inc.). First-strand cDNA was synthesized using a PrimeScript RT kit (cat. no. RR047A; Takara Bio, Inc.), and qPCR was conducted using PrimeScript Master Mix (cat. no. RR036A; Takara Bio, Inc.). The reaction conditions used in the experiment were as follows: Pre-denaturation at 95°C for 30 sec, followed by 40 cycles of 95°C for 5 sec and 60°C for 20 sec. The relative mRNA expression levels were calculated according to the 2^{- $\Delta\Delta$ C_q} method (22). GAPDH was used as the internal reference.

Table I. Primer sequences.

Gene name	Primer sequence (5'→3')
GAPDH	F: TGTGTCCGTCGTGGATCTGA R: TTGCTGTTGAAGTCGCAGGAG
SIRT1	F: ACAGTGAGAAAATGCTGGC R: GCCACTGTCACTGTTACTGC
PGC-1 α	F: AGCAGAAAGCAATTGAAGAG R: AGGTGTAACGGTAGGTGATG

F, forward; R, reverse; PGC-1 α , peroxisome proliferator-activated receptor γ coactivator-1 α ; SIRT1, sirtuin 1.

Western blotting. Mouse gastrocnemius muscle tissues or C2C12 cells were processed to form suspensions using RIPA lysis buffer (Santa Cruz Biotechnology, Inc.) containing 1% PMSF (Beyotime Institute of Biotechnology) to extract the total protein. The solutions were centrifuged at 10,000 x g for 15 min, and the protein concentration of the supernatant was determined using the BCA method. Then, 30 μ g of each sample was separated via 12% SDS-PAGE, blotted onto PVDF membranes and blocked with 5% skim milk at room temperature for 1 h. The membranes were then washed three times with TBS-0.1% Tween-20 (TBST), and primary antibodies against IRS1 (1:1,000; cat. no. 2382; Cell Signaling Technology, Inc.), phosphorylated (p)-IRS1 (1:1,000; cat. no. 2385; Cell Signaling Technology, Inc.), PI3K (1:1,000; cat. no. 4255; Cell Signaling Technology, Inc.), p-PI3K (1:1,000; cat. no. 4228; Cell Signaling Technology, Inc.), AKT (1:1,000; cat. no. 4691; Cell Signaling Technology, Inc.), p-AKT (1:1,000; cat. no. 4060; Cell Signaling Technology, Inc.), GLUT4 (1:1,000; cat. no. 2213S; Cell Signaling Technology, Inc.), SIRT1 (1:1,000; cat. no. 2496; Cell Signaling Technology, Inc.), PGC-1 α (1:1,000; cat. no. 2178; Cell Signaling Technology, Inc.) and GAPDH (1:1,000; cat. no. 5174; Cell Signaling Technology, Inc.) were incubated with the membrane for 2 h at room temperature. After being washed three times with TBST, the membranes were incubated with an anti-rabbit HRP-labeled secondary antibody (1:1,000; cat. no. 7074; Cell Signaling Technology, Inc.) or anti-mouse HRP-labeled secondary antibody (1:1,000; cat. no. 7076S; Cell Signaling Technology, Inc.) for 1 h at room temperature. The protein bands were visualized using an ECL chemiluminescence detection kit (EMD Millipore) under a gel imaging system, and ImageJ software (v1.6.0; National Institutes of Health) was used to perform densitometric analysis.

Statistical analysis. All data were statistically analyzed using SPSS (version 22.0; IBM Corp.) and expressed as the mean \pm SD. One-way analysis of variance (ANOVA) with Tukey's multiple comparison post hoc test were used to compare the data among groups, and $P < 0.05$ was considered to indicate a statistically significant difference. GraphPad Prism 8.0 (GraphPad Software, Inc.) and SPSS was used to draw the graphs.

Results

MNAM improves IR in T2DM mice. The body weights of mice in the DM group were increased significantly throughout the 8-week feeding period compared with the control group (Fig. 1A), and the levels of FBG (Fig. 1B) and FINS (Fig. 1C) were also elevated. When different concentrations of MNAM were added to the diet, the body weight gain of ob/ob mice was attenuated (Fig. 1A), as were the increases in FBG and FINS levels (Fig. 1B and C). These results suggested that MNAM may reduce the body weights, FBG and FINS of T2DM mice. Furthermore, IR was analyzed according to the HOMA-IR and QUICKI equations. The results showed that mice in the DM group exhibited the highest HOMA-IR and the lowest QUICKI values (Fig. 1D), compared with the results observed in the control and CMNAMH groups. The HOMA-IR levels of ob/ob mice fed with different concentrations of MNAM were decreased, whereas the QUICKI indexes were increased ($P < 0.05$ vs. DM group). These results indicated that MNAM could improve IR in T2DM mice.

MNAM reduces the TG content in the skeletal muscle of T2DM mice. It was shown that the highest TG content was observed in ob/ob mice in DM group (Fig. 2). The TG content in the DM group was significantly increased compared with the control group. Interestingly, both of DMNAML and DMNAMH were shown to significantly reduce the TG content of skeletal muscle in T2DM mice ($P < 0.05$ vs. DM). Moreover, no statistical differences were found in the TG levels between the DMNAML and DMANAML groups. These results suggest that MNAM could significantly decrease the TG level in T2DM mice skeletal muscle tissue.

Effects of MNAM on the insulin signaling pathway in skeletal muscle. In the DM group, no significant changes were observed in IRS1 expression; however, the phosphorylation of IRS1 was downregulated compared with control group, which was accompanied by the downregulation of the phosphorylation of PI3K and AKT (Fig. 3A). Moreover, the decrease of GLUT4 expression in skeletal muscle in the DM group was also observed compared with the control group (Fig. 3B). When MNAM was applied, the activities of IRS1, PI3K and AKT were increased, in addition to the expression of GLUT4.

MNAM activates the SIRT1/PGC-1 α pathway in the skeletal muscle of T2DM mice. In the DM group, the protein (Fig. 4A) and mRNA (Fig. 4B) expression levels of SIRT1 were decreased compared with control group, with the expression of its downstream regulator, PGC-1 α , also inhibited. After being fed with 1% MNAM, the expression levels of SIRT1 and PGC-1 α mRNA and protein were significantly elevated in the skeletal muscle of ob/ob mice.

Effects of inhibiting SIRT1 on the effects of MNAM in insulin-resistant myocytes. The regulatory mechanisms of the SIRT1/PGC-1 α pathway in IR were further investigated *in vitro*. An *in vitro* IR model was established by exposing C2C12 myoblasts to PA. It was observed that the expression levels of SIRT1 and PGC-1 α protein (Fig. 5A) and mRNA (Fig. 5B) in the PA-exposed group were decreased compared

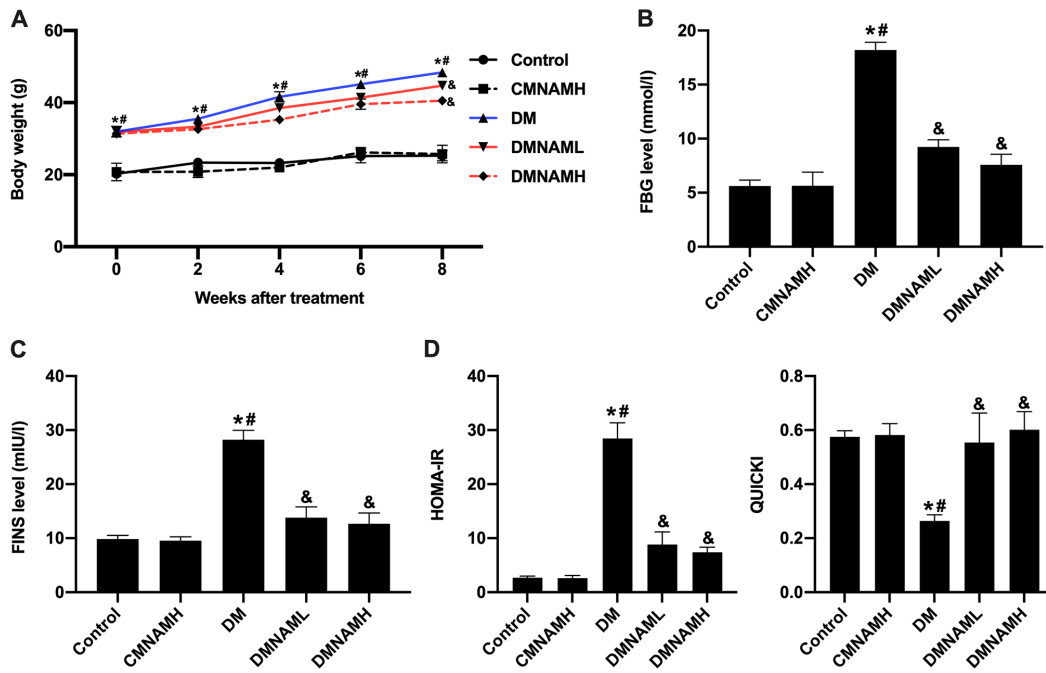


Figure 1. MNAM improves insulin resistance in type 2 DM mice. (A) Body weights of mice in each group. (B) FBG of mice in each group. (C) FINS of mice in each group. (D) HOMA-IR and QUICKI of mice in each group. *P<0.05 vs. control; #P<0.05 vs. CMNAMH; &P<0.05 vs. DM. DM, diabetes mellitus; MNAM, N1-methylnicotinamide; CMNAMH, control treated with high dose of MNAM; DMNAML, DM group treated with low dose of MNAM; DMNAMH, DM group treated with high dose of MNAM; FBG, fasting blood glucose; FINS, fasting insulin; HOMA-IR, homeostatic model assessment for insulin resistance; QUICKI, quantitative insulin resistance check index.

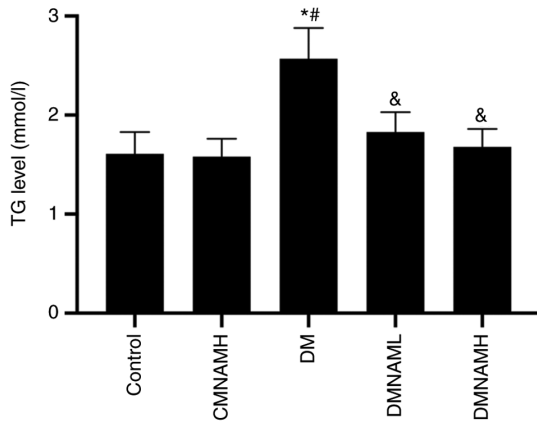


Figure 2. MNAM decreases the TG content in the skeletal muscle of type 2 DM mice. TG content of mice in each group as determined via ELISA. *P<0.05 vs. control; #P<0.05 vs. CMNAMH; &P<0.05 vs. DM. DM, diabetes mellitus; MNAM, N1-methylnicotinamide; CMNAMH, control treated with high dose of MNAM; DMNAML, DM group treated with low dose of MNAM; DMNAMH, DM group treated with high dose of MNAM; TG, triglyceride.

with the control, which was consistent with the results obtained *in vivo*. MNAM application activated the SIRT1/PGC-1 α signaling pathway, increased glucose consumption (Fig. 5C), promoted the phosphorylation of IRS1, PI3K and AKT, and increased GLUT4 expression in muscle cells (Fig. 5D), suggestive of attenuated IR. When EX527, a SIRT1 inhibitor, was administered to C2C12 cells, glucose consumption was inhibited, as the residual glucose content was significantly increased (P<0.05 vs. PM), PGC-1 α expression was decreased, the phosphorylation levels of IRS1, PI3K and AKT were inhibited,

and the expression of GLUT4 in muscle cells was downregulated (Fig. 5E), suggesting that MNAM may improve IR by activating the SIRT1/PGC-1 α signaling pathway.

Discussion

The leading causes of T2DM are IR and islet β cell dysfunction (23). IR typically occurs prior to islet β cell injury. When islet β cells can no longer compensate for IR by increasing insulin secretion, impairments in glucose tolerance occur and gradually develops into DM (24). In the present study, a mouse model of T2DM was established according to the protocols described by Hong *et al* (11), who fed cohorts of wild-type C57BL/6J mice with a saturated-fat diet supplemented with different doses of MNAM (0.3% and 1%) for several weeks without adverse effects. Our previous study showed that MNAM could improve hepatic insulin sensitivity by activating SIRT1 and inhibiting FOXO1 acetylation (12). In the present study, it was demonstrated that MNAM could reduce body weight increases in ob/ob T2DM mice and decrease the levels of FBG and FINS in serum. Moreover, MNAM regulated insulin signal transduction, reduced lipid deposition and promoted glucose utilization in skeletal muscle, resulting in the attenuation of IR in the skeletal muscle of T2DM mice. The mechanism of action was suggested to involve activation of the SIRT1/PGC-1 α pathway. The present and aforementioned previous studies indicated that MNAM performed similar functions in different tissues in T2DM mice.

Skeletal muscle is the most essential tissue for maintaining glucose homeostasis in the body, and is responsible for 80% of insulin-induced glucose uptake and utilization under normal conditions (25). One of the main effects of

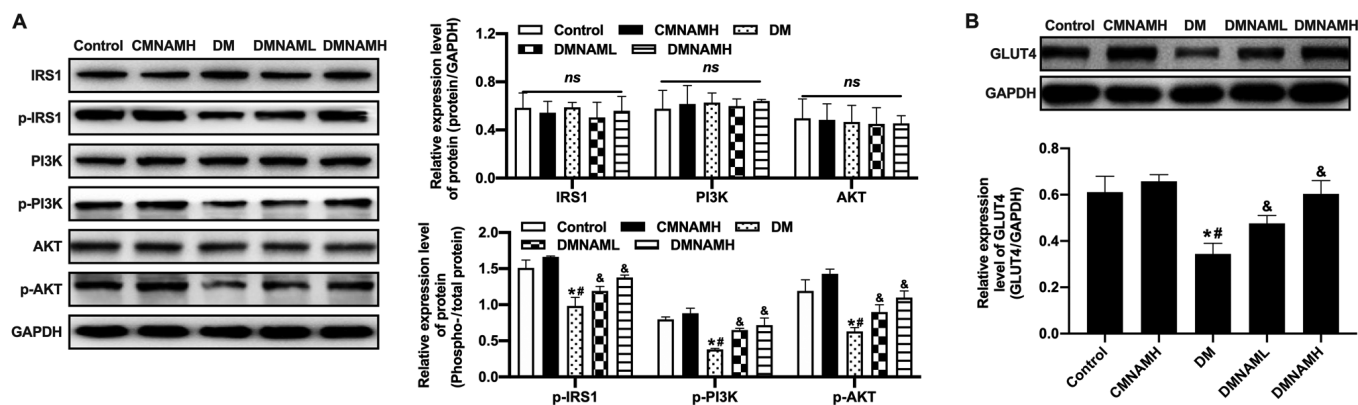


Figure 3. Effect of MNAM on the insulin signaling pathway in skeletal muscle. (A) Western blotting was used to detect the levels of p-IRS1/IRS1, p-PI3K/PI3K and p-AKT/AKT. (B) Western blotting was used to determine the protein expression of GLUT4. * $P < 0.05$ vs. control; # $P < 0.05$ vs. CMNAMH; & $P < 0.05$ vs. DM. DM, diabetes mellitus; MNAM, N1-methylnicotinamide; CMNAMH, control treated with high dose of MNAM; DMNAML, DM group treated with low dose of MNAM; DMNAMH, DM group treated with high dose of MNAM; IRS1, insulin receptor substrate 1; p, phosphorylated; GLUT4, glucose transporter 4; ns, not significant.

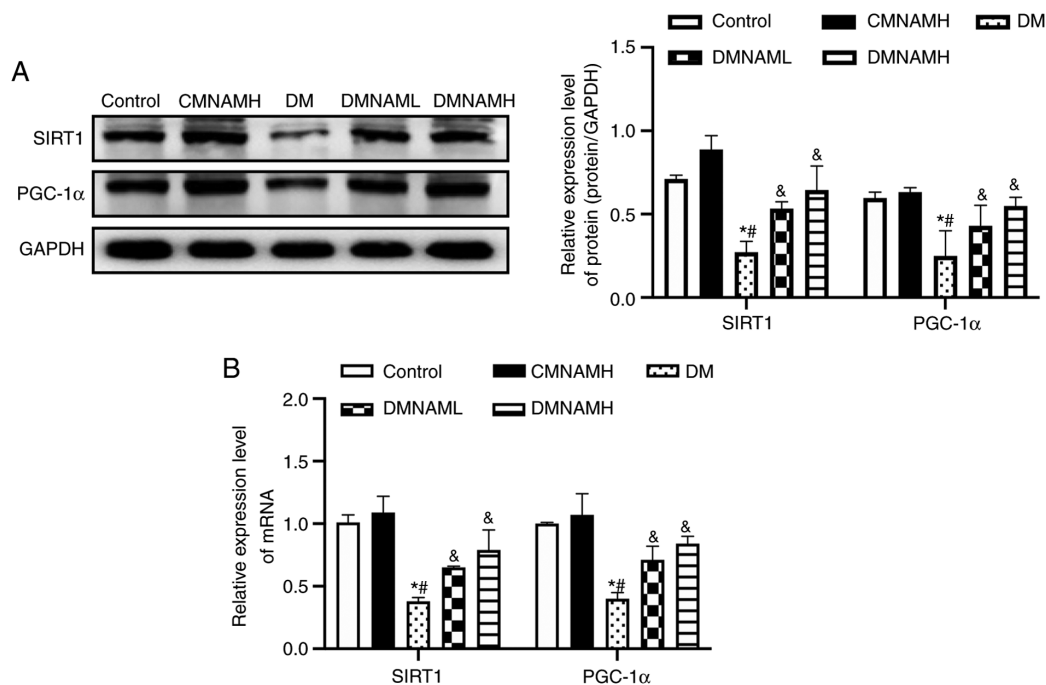


Figure 4. MNAM activates the SIRT1/PGC-1 α signaling pathway in the skeletal muscle of type 2 DM mice. (A) Western blotting was used to quantify the protein expression of SIRT1 and PGC-1 α . (B) Reverse transcription-quantitative PCR were used to determine the mRNA expression of SIRT1 and PGC-1 α . * $P < 0.05$ vs. control; # $P < 0.05$ vs. CMNAMH; & $P < 0.05$ vs. DM. DM, diabetes mellitus; MNAM, N1-methylnicotinamide; CMNAMH, control treated with high dose of MNAM; DMNAML, DM group treated with low dose of MNAM; DMNAMH, DM group treated with high dose of MNAM; SIRT1, sirtuin 1; PGC-1 α , peroxisome proliferator-activated receptor γ coactivator-1 α .

IR in skeletal muscle is to increase the lipid content of muscle cells (26). When the levels of free fatty acids exceed the oxidation capability of tissues, excessive fatty acids are deposited in skeletal muscle as TGs, which affects the occurrence and development of IR (26). In the present study, it was found that the TG content in gastrocnemius muscle in the DM group was notably elevated compared with in the other four groups. It was further observed that MNAM intervention decreased the TG content in gastrocnemius muscles of ob/ob mice to normal levels, indicating that MNAM attenuated the IR of skeletal muscle by improving lipid metabolism in skeletal muscle.

When insulin is bound to membrane receptors located on skeletal muscle cells, insulin signal cascade reactions are triggered, catalyzing the phosphorylation of IRS1 (27). p-IRS1 immediately combines with PI3K and subsequently induces its downstream factor, AKT (28). As the uninduced PI3K signaling pathway regulates the metabolism of glucose, fat and protein, the decreased induction of IRS1 signaling may promote IR (29). GLUT4 is a downstream regulator of PI3K and a key protein that controls glucose uptake and glycogen metabolism (30). GLUT4 expression is decreased in patients with T2DM, which reduces the uptake and utilization of glucose (31). Therefore, the IRS1/PI3K/AKT/GLUT4 signaling

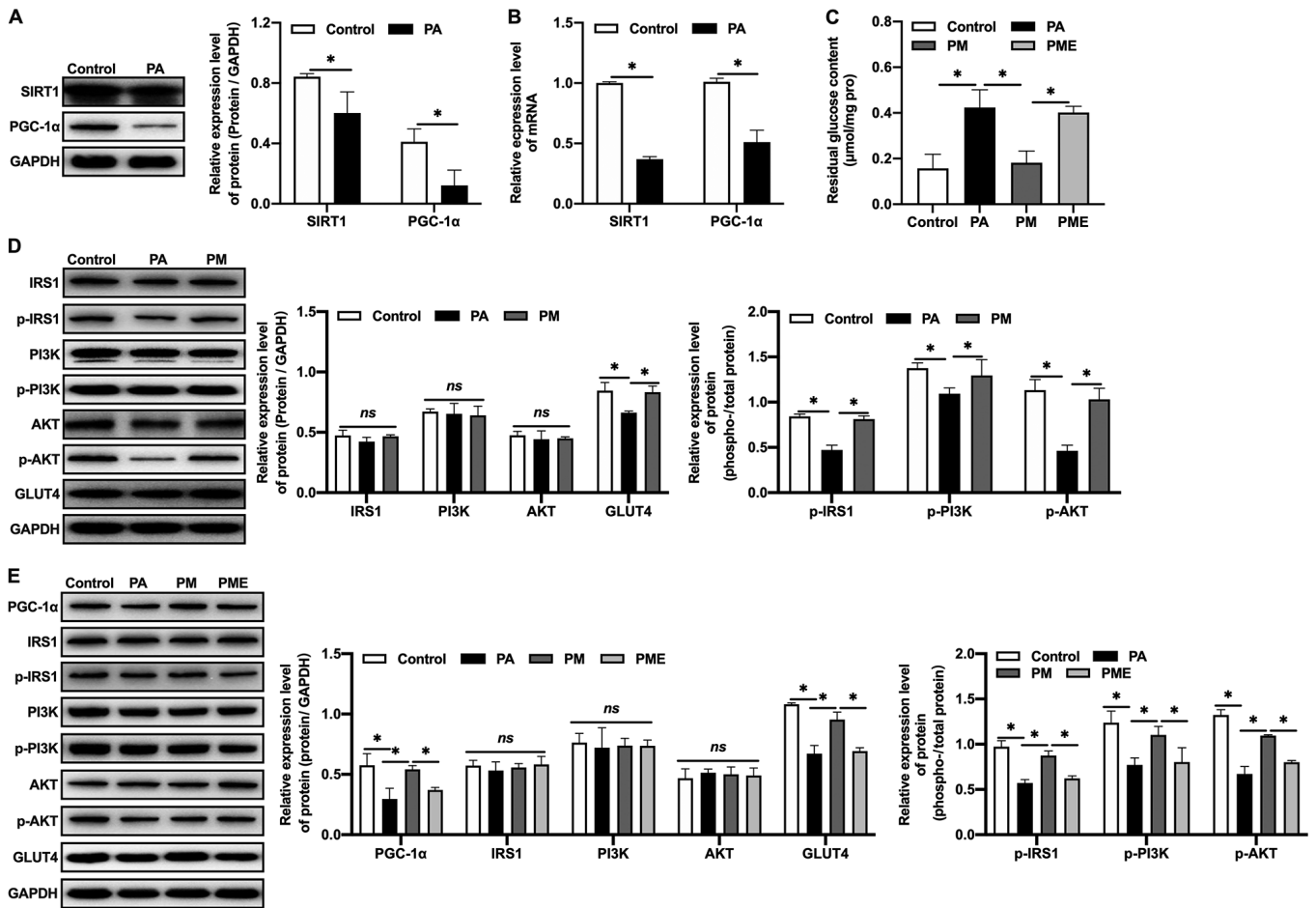


Figure 5. Effects of inhibiting SIRT1 on MNAM-induced improvements in insulin resistance in insulin-resistant myocytes. (A) Western blotting was used to detect the protein expression levels of SIRT1 and PGC-1 α . (B) Reverse transcription-quantitative PCR was used to quantify the mRNA expression of SIRT1 and PGC-1 α . (C) Residual glucose content. (D) Western blotting was used to determine the levels of p-IRS1/IRS1, p-PI3K/PI3K and p-AKT/AKT. (E) Western blotting was used to detect the levels of PGC-1 α , p-IRS1/IRS1, p-PI3K/PI3K, p-AKT/AKT and GLUT4 following SIRT1 inhibition. * P <0.05. PA, palmitic acid; MNAM, N1-methylnicotinamide; PM, PA + MNAM; PME, PA + MNAM + EX527; SIRT1, sirtuin 1; PGC-1 α , peroxisome proliferator-activated receptor γ coactivator-1 α ; IRS1, insulin receptor substrate 1; p, phosphorylated; GLUT4, glucose transporter 4; ns, not significant.

pathway serves an important role in insulin signal transduction in skeletal muscle. Any disruption within this pathway may reduce the sensitivity of skeletal muscle to insulin, leading to dysfunctional glucose uptake and utilization, and reduced glucose tolerance.

It was found that the phosphorylation levels of IRS1, PI3K, and AKT in skeletal muscle of DM group mice were decreased, and GLUT4 expression was downregulated, compared with control group mice, suggesting that there was abnormal insulin signal transduction in skeletal muscle in T2DM mice. However, the levels of p-IRS1, p-PI3K, p-AKT and GLUT4 were increased in T2DM mice that were administered MNAM, suggesting that MNAM improved IR by restoring insulin signal transduction in skeletal muscle.

SIRT1 plays a vital role in glucose homeostasis and energy metabolism; previous studies reported that SIRT1 can improve IR in the liver, skeletal muscle and adipose tissues, and protect pancreatic β cells (32,33). Muscle biopsies from patients with T2DM showed decreased expression of SIRT1, and overexpression of SIRT1 could reduce IR in skeletal muscle cells (34). SIRT1 in skeletal muscle can activate the insulin signaling pathway, and specifically increase the phosphorylation of

PI3K/AKT (35). It was reported that SIRT1 in skeletal muscle also affects the phosphorylation of IRS1 and GLUT4 recruitment, and can regulate glycolipid metabolism via direct or indirect participation in insulin signal transduction (36,37).

In the present study, it was reported that the levels of p-IRS1, p-PI3K, p-AKT and GLUT4, as well as glucose uptake, were significantly decreased in skeletal muscle tissue and muscle cells during IR. It was also demonstrated that MNAM intervention could increase the phosphorylation levels of IRS1, PI3K and AKT, the expression of GLUT4, and glucose uptake and utilization. When SIRT1 was inhibited, the expression of downstream PGC-1 α was also inhibited, as well the phosphorylation levels of IRS1, PI3K and AKT, and the expression of GLUT4. The residual glucose content was increased, indicating that the glucose consumption of muscle cells was decreased. It was further suggested that MNAM modulated the insulin signaling pathway, improved IR and increased glucose utilization in skeletal muscle and muscle cells, which was attenuated by inhibition of SIRT1. The results indicated that MNAM regulated IR in skeletal muscle via the SIRT1/PGC-1 α signaling pathway.

In conclusion, the results suggested that MNAM reduced body weight gain in obese T2DM mice, decreased FBG and

FINS levels, and regulated insulin signal transduction in skeletal muscle, reducing lipid build-up and promoting glucose utilization, and resulting in the improvement of IR in the skeletal muscle of T2DM mice. These improvements in functions may occur due to the MNAM-regulated activation of the SIRT1/PGC-1 α signaling pathway.

Acknowledgements

Not applicable.

Funding

This work was supported by Young Scientists of the National Science Foundation of China (grant no. 81600644).

Availability of data and materials

The datasets used and/or analyzed during the current study are available from the corresponding author on reasonable request.

Authors' contributions

LL designed the study. YC performed the animal experiments. JZ performed the cell experiments. YC and CL analyzed and interpreted the data. YC and PL performed the western blotting and RT-qPCR analyses. YC was a major contributor to the writing of the manuscript. YC and LL confirm the authenticity of all the raw data. All authors read and approved the final manuscript.

Ethics approval and consent to participate

The experimental protocols were approved by the Animal Ethics Committee of Shengjing Hospital of China Medical University (approval no. 2016PS340K).

Patient consent for publication

Not applicable.

Competing interests

The authors declare that they have no competing interests.

References

- Barnett R: Type 2 diabetes. *Lancet* 394: 557, 2019.
- Saeedi P, Petersohn I, Salpea P, Malanda B, Karuranga S, Unwin N, Colagiuri S, Guariguata L, Motala AA, Ogurtsova K, *et al*: Global and regional diabetes prevalence estimates for 2019 and projections for 2030 and 2045: Results from the international diabetes federation diabetes atlas, 9(th) edition. *Diabetes Res Clin Pract* 157: 107843, 2019.
- Weyer C, Tataranni PA, Bogardus C and Pratley RE: Insulin resistance and insulin secretory dysfunction are independent predictors of worsening of glucose tolerance during each stage of type 2 diabetes development. *Diabetes Care* 24: 89-94, 2001.
- Hernandez-Carretero A, Weber N, LaBarge SA, Peterka V, Doan NYT, Schenk S and Osborn O: Cysteine- and glycine-rich protein 3 regulates glucose homeostasis in skeletal muscle. *Am J Physiol Endocrinol Metab* 315: E267-E78, 2018.
- Amati F: Revisiting the diacylglycerol-induced insulin resistance hypothesis. *Obes Rev* 13 (Suppl 2): S40-S50, 2012.
- Esteves JV, Enguita FJ and Machado UF: MicroRNAs-mediated regulation of skeletal muscle GLUT4 expression and translocation in insulin resistance. *J Diabetes Res* 2017: 7267910, 2017.
- Guo X, Sun W, Luo G, Wu L, Xu G, Hou D, Hou Y, Guo X, Mu X, Qin L and Liu T: Panax notoginseng saponins alleviate skeletal muscle insulin resistance by regulating the IRS1-PI3K-AKT signaling pathway and GLUT4 expression. *FEBS Open Bio* 9: 1008-1019, 2019.
- Nikas IP, Paschou SA and Ryu HS: The role of nicotinamide in cancer chemoprevention and therapy. *Biomolecules* 10: 477, 2020.
- Knip M, Douek IF, Moore WP, Gillmor HA, McLean AE, Bingley PJ and Gale EA; European Nicotinamide Diabetes Intervention Trial Group: Safety of high-dose nicotinamide: A review. *Diabetologia* 43: 1337-1345, 2000.
- Nejabati HR, Mihanfar A, Pezeshkian M, Fattahi A, Latifi Z, Safaie N, Valiloo M, Jodati AR and Nouri M: N1-methylnicotinamide (MNAM) as a guardian of cardiovascular system. *J Cell Physiol* 233: 6386-6394, 2018.
- Hong S, Moreno-Navarrete JM, Wei X, Kikukawa Y, Tzamelis I, Prasad D, Lee Y, Asara JM, Fernandez-Real JM, Maratos-Flier E and Pissios P: Nicotinamide N-methyltransferase regulates hepatic nutrient metabolism through Sirt1 protein stabilization. *Nat Med* 21: 887-894, 2015.
- Zhang J, Chen Y, Liu C, Li L and Li P: N(1)-methylnicotinamide improves hepatic insulin sensitivity via activation of SIRT1 and inhibition of FOXO1 acetylation. *J Diabetes Res* 2020: 1080152, 2020.
- Gu C, Zeng Y, Tang Z, Wang C, He Y, Feng X and Zhou L: Astragalus polysaccharides affect insulin resistance by regulating the hepatic SIRT1-PGC-1 α /PPAR α -FGF21 signaling pathway in male Sprague Dawley rats undergoing catch-up growth. *Mol Med Rep* 12: 6451-6460, 2015.
- Waldman M, Nudelman V, Shainberg A, Abraham NG, Kornwoski R, Aravot D, Arad M and Hochhauser E: PARP-1 inhibition protects the diabetic heart through activation of SIRT1-PGC-1 α axis. *Exp Cell Res* 373: 112-118, 2018.
- Cheng CF, Ku HC and Lin H: PGC-1 α as a pivotal factor in lipid and metabolic regulation. *Int J Mol Sci* 19: 3447, 2018.
- Guilford BL, Parson JC, Grote CW, Vick SN, Ryals JM and Wright DE: Increased FNDC5 is associated with insulin resistance in high fat-fed mice. *Physiol Rep* 5: e13319, 2017.
- Lagouge M, Argmann C, Gerhart-Hines Z, Meziane H, Lerin C, Daussin F, Messadeq N, Milne J, Lambert P, Elliott P, *et al*: Resveratrol improves mitochondrial function and protects against metabolic disease by activating SIRT1 and PGC-1 α . *Cell* 127: 1109-1122, 2006.
- Drel VR, Mashtalir N, Ilnytska O, Shin J, Li F, Lyzogubov VV and Obrosova IG: The leptin-deficient (ob/ob) mouse: A new animal model of peripheral neuropathy of type 2 diabetes and obesity. *Diabetes* 55: 3335-3343, 2007.
- Tang Q, Li X, Song P and Xu L: Optimal cut-off values for the homeostasis model assessment of insulin resistance (HOMA-IR) and pre-diabetes screening: Developments in research and prospects for the future. *Drug Discov Ther* 9: 380-385, 2015.
- Shojaeian Z, Sadeghi R and Latifnejad Roudsari R: Calcium and vitamin D supplementation effects on metabolic factors, menstrual cycles and follicular responses in women with polycystic ovary syndrome: A systematic review and meta-analysis. *Caspian J Intern Med* 10: 359-369, 2019.
- Yaffe D and Saxel O: Serial passaging and differentiation of myogenic cells isolated from dystrophic mouse muscle. *Nature* 270: 725-727, 1977.
- Livak KJ and Schmittgen TD: Analysis of relative gene expression data using real-time quantitative PCR and the 2(-Delta Delta C(T)) method. *Methods* 25: 402-408, 2001.
- Shin JJ, Lee EK, Park TJ and Kim W: Damage-associated molecular patterns and their pathological relevance in diabetes mellitus. *Ageing Res Rev* 24: 66-76, 2015.
- Ortega A, Berná G, Rojas A, Martín F and Soria B: Gene-diet interactions in type 2 diabetes: The chicken and egg debate. *Int J Mol Sci* 18: 1188, 2017.
- Carnagarin R, Dharmarajan AM and Dass CR: Molecular aspects of glucose homeostasis in skeletal muscle-A focus on the molecular mechanisms of insulin resistance. *Mol Cell Endocrinol* 417: 52-62, 2015.
- Beaudry KM and Devries MC: Sex-based differences in hepatic and skeletal muscle triglyceride storage and metabolism (1). *Appl Physiol Nutr Metab* 44: 805-813, 2019.

27. Yu N, Fang X, Zhao D, Mu Q, Zuo J, Ma Y, Zhang Y, Mo F, Zhang D, Jiang G, *et al*: Anti-diabetic effects of Jiang Tang Xiao Ke granule via PI3K/Akt signalling pathway in type 2 diabetes KK Δ y mice. *PLoS One* 12: e0168980, 2017.
28. Gao Y, Zhang M, Zhang R, You L, Li T and Liu RH: Whole grain brown rice extrudate ameliorates the symptoms of diabetes by activating the IRS1/PI3K/AKT insulin pathway in db/db mice. *J Agric Food Chem* 67: 11657-11664, 2019.
29. Huang X, Liu G, Guo J and Su Z: The PI3K/AKT pathway in obesity and type 2 diabetes. *Int J Biol Sci* 14: 1483-1496, 2018.
30. Richter EA and Hargreaves M: Exercise, GLUT4, and skeletal muscle glucose uptake. *Physiol Rev* 93: 993-1017, 2013.
31. Piątkiewicz P, Bernat-Karpińska M, Miłek T, Rabijewski M and Rosiak E: NK cell count and glucotransporter 4 (GLUT4) expression in subjects with type 2 diabetes and colon cancer. *Diabetol Metab Syndr* 8: 38, 2016.
32. Yu L, Chen JF, Shuai X, Xu Y, Ding Y, Zhang J, Yang W, Liang X, Su D and Yan C: Artesunate protects pancreatic beta cells against cytokine-induced damage via SIRT1 inhibiting NF- κ B activation. *J Endocrinol Invest* 39: 83-91, 2016.
33. Zhou S, Tang X and Chen HZ: Sirtuins and insulin resistance. *Front Endocrinol (Lausanne)* 9: 748, 2018.
34. Kitada M, Ogura Y, Monno I and Koya D: Sirtuins and type 2 diabetes: Role in inflammation, oxidative stress, and mitochondrial function. *Front Endocrinol (Lausanne)* 10: 187, 2019.
35. Lee D and Goldberg AL: SIRT1 protein, by blocking the activities of transcription factors FoxO1 and FoxO3, inhibits muscle atrophy and promotes muscle growth. *J Biol Chem* 288: 30515-30526, 2013.
36. Sin TK, Yu AP, Yung BY, Yip SP, Chan LW, Wong CS, Rudd JA and Siu PM: Effects of long-term resveratrol-induced SIRT1 activation on insulin and apoptotic signalling in aged skeletal muscle. *Acta Diabetol* 52: 1063-1075, 2015.
37. Manna P, Achari AE and Jain SK: 1,25(OH)(2)-vitamin D(3) upregulates glucose uptake mediated by SIRT1/IRS1/GLUT4 signaling cascade in C2C12 myotubes. *Mol Cell Biochem* 444: 103-108, 2018.